Soft Endoluminal Robots Propelled by Rotating Magnetic Dipole Fields

Lan N. Pham, *Student Member, IEEE*, Jake A. Steiner, *Student Member, IEEE*, Kam K. Leang, *Senior Member, IEEE*, and Jake J. Abbott, *Senior Member, IEEE*

***Abstract*—Medical procedures often involve a device moving through a natural lumen of the human body (e.g., intestines, blood vessels). However, with existing technology, it is difficult, impossible, or traumatic to reach certain locations. In this article, we present a magnetically actuated soft-robotic concept for use in endoluminal applications (e.g., capsule endoscopes and catheters). The soft endoluminal robot is a simple device comprising two or more permanent magnets, axially magnetized and embedded co-axially with alternating polarity in a compliant body, with an optional internal lumen, actuated by an external rotating magnetic dipole field. We use simulations to elucidate the actuation concept's underlying physics and, combined with experiments, demonstrate how the proposed concept outperforms other potential variations. We experimentally demonstrate the robustness to misalignment between the soft robot and the applied field, enabling operation in different applications without precise knowledge of the robot's orientation or precise control of the actuator dipole field. Experiments are then performed inside a synthetic bowel to compare capsule-endoscope-size robots and multi-component robots formed by connecting multiple capsule-endoscope-size robots axially. Finally, experiments in a synthetic stomach show how the concept lends itself to directed self-assembly in the stomach, thus creating robots that are larger than could be swallowed.**

***Index Terms*—Medical robotics, soft robotics, magnetic actuation.**

I. Introduction

A WIDE variety of medical procedures involve a device moving through a natural lumen of the human body, such as a blood vessels or the intestines. However, in many cases, existing technology is insufficient to enable clinicians to achieve their desired goals. For example, consider insertion of catheters into the vasculature of the brain, where passages are narrow and intricate, requiring multiple catheters to be inserted, putting the lumen at risk of puncture [1]. Also, consider colonoscopy, which is a crucial screening procedure that is associated with discomfort, requires sedation, and is sometimes incomplete (unable to reach the cecum). Loeve *et al.* [2] described a paradoxical problem of flexible endoscopy: endoscopes are both too flexible and too stiff. They described how stiffness is necessary to perform an insertion successfully, yet softness is required to allow the device to adapt to unknown soft-tissue environments to ensure the lumen's safety. However, there is an underlying assumption here that the device is pushed through the lumen from its proximal end, and must steer and conform to the geometry of the lumen. One solution to circumvent this perceived paradox is to create devices that can assist in their own propulsion in order to reduce the proximal insertion forces that are required [3]–[5]. Untethered devices, such as robotic capsule endoscopes, must carry their own intrinsic propulsion system, which has taken various forms ranging from mechatronic (e.g., insect-like legs, rectilinear traveling wave) to magnetic [5], [6]. Magnetic actuation is particularly attractive because much of the footprint for the robotic system is contained in the external magnetic system, which enables the *in vivo* device to be both simpler and smaller than would be possible otherwise.

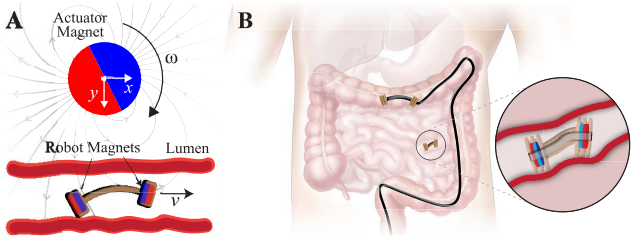

Fig. 1. The proposed magnetic-actuation concept. (**A**) The soft robot comprises a compliant continuum structure with two or more co-axially embedded magnets with alternating polarity. When the robot is subjected to an external rotating dipole field, the result is a periodic gait that propels the robot forward. In the nominal configuration (shown), the local lumen axis, external-magnet rotation axis, and the displacement vector from the external magnet to the robot are mutually orthogonal. (**B**) The soft robot has potential uses in a variety of applications, such as tethered catheter or endoscope procedures or in untethered motion through lumens of the body. The robot can contain a central lumen to permit the passage of fluids and objects.

In this article, we describe a type of magnetic actuation designed explicitly for use with soft endoluminal robots (Fig. 1). This work builds upon our initial study described in [7]. The robot comprises a compliant continuum structure with two or more co-axially embedded permanent magnets with alternating magnetic polarity and axial magnetization. Polymer material surrounds the embedded magnets to serve as feet on each end of the robot. When subjected to an external rotating magnetic dipole field (e.g., the field generated by

Manuscript received July 27, 2020; revised September 18, 2020; accepted September 24, 2020. Date of publication September 30, 2020; date of current version November 20, 2020. This article was recommended for publication by Associate Editor A. Menciassi and Editor P. Dario upon evaluation of the reviewers' comments. This work was supported by the National Science Foundation under Grant 1830958. *(Lan N. Pham and Jake A. Steiner contributed equally to this work.) (Corresponding author: Lan N. Pham.)*

The authors are with the Department of Mechanical Engineering and Robotics Center, University of Utah, Salt Lake City, UT 84112 USA (e-mail: lan.pham@utah.edu; jake.steiner@utah.edu; kam.k.leang@utah.edu; jake.abbott@utah.edu).

This article has supplementary downloadable material available at https://ieeexplore.ieee.org, provided by the authors.

Digital Object Identifier 10.1109/TMRB.2020.3027871

2576-3202 © 2020 IEEE. Personal use is permitted, but republication/redistribution requires IEEE permission.
See https://www.ieee.org/publications/rights/index.html for more information.

rotating a permanent magnet whose dipole is orthogonal to the axis of rotation), a periodic gait emerges that propels the robot forward with locomotion that typically manifests as an inchworm-like gait. The body bends to bring the feet closer together and straightens out to push the feet apart. The two points of contact at the feet alternate anchoring and releasing, relying on the asymmetry in reaction forces and resulting friction induced on the two points of contact.

The sign convention demonstrating a positive actuator-magnet rotation, ω, leading to positive robot velocity, v, is depicted in Fig. 1(A); if the rotation of the applied magnetic field is reversed, the robot's traveling direction is also reversed. The robot's speed is a function of the actuator magnet's angular velocity. Since this actuation concept is wireless, and because it has no internal moving parts beyond mechanical compliance, it can be fabricated at a wide range of sizes.

The robot concept is specialized for endoluminal applications in four respects:

1) The radial symmetry of the robot eliminates the challenges of localizing and controlling the roll orientation of the robot within the lumen.
2) The bilateral symmetry of the robot ensures that locomotion is not biased toward one direction along the lumen.
3) The robot's embedded magnets can be fabricated with an annular geometry, without interfering with the actuation. This enables the creation of an internal lumen to enable fluids to pass through (e.g., so as to not fully obstruct a blood vessel that the robot is crawling through).
4) The robot is actuated by a nonuniform magnetic dipole field. Placing a dipole-field source adjacent to a patient is easier than surrounding a patient with electromagnetic coils required to generate uniform magnetic fields of equivalent strength.

We envision a variety of possible applications for the proposed concept: an untethered soft robot such as a capsule endoscope, an untethered multi-component soft robot composed of individual robots chained together *in vivo* via (directed) self-assembly, and a continuum device such as a catheter with the soft-robot component at its distal end or with multiple such components distributed along its length.

There are four main contributions of our work. First is an elucidation of the underlying physics behind the actuation, with numerical confirmation of the experimental trends observed in [7], using a simulation developed in [8]. Second is experimental demonstrations of the robustness of the performance of the robot to misalignment error between the soft robot and the applied field. Third is experiments in a synthetic bowel segment using a capsule-size robot and a multi-component robot formed by connecting two capsule-sized robots. Finally, the fourth is an *in vitro* study demonstrating the concept's potential for directed self-assembly in the stomach, which would enable modular soft endoluminal robots for use in the gastrointestinal (GI) tract that are larger than could be swallowed.

II. Related Works

The field of soft continuum robotics has received a great deal of interest in recent years [9]–[12]. However, a critical survey of the literature reveals that many existing soft manipulator technologies do not scale well for the size required to navigate the natural lumina of the body. As a result, we shall focus on prior works that have attempted to address medical applications. In the design of continuum manipulators for medical applications [13], we see a pervasive theme of designing robots with high-degree-of-freedom controllable kinematics. The essential idea is to enable the robot to actively conform to some desired path, where any compliance is primarily used to accommodate robot limitations and modeling errors. In addition, the manipulators are typically designed to work in free space, which requires some degree of stiffness. We are particularly interested in robots that are specialized for use in a lumen—robots that can passively conform to the tortuous path they must navigate, but need not support their weight in free space.

Several groups have described magnetic actuation methods to enable locomotion through a lumen, typically motivated by medical applications. Catheter methods typically access the vascular system of the body. Magnetic actuation of catheters has been around since the 1950s [4], [14], when its utility was demonstrated in the cerebral artery, the bronchial anatomy, and the heart. Recent work in this area has considered ferromagnetic soft-continuum robotic catheters at even smaller scales [15]. To access the GI tract, both pushed continuum devices and untethered capsule devices are used. Both have received significant attention in recent years, motivated by the desire to improve both the quality of GI-tract screening procedures and the patient's experience [5], [6]. Scope devices are currently unable to reach past the cecum when approaching from the anus, or past the duodenum when approaching from the mouth [16]. Capsule devices can reach the entire GI tract but have neither the control to investigate regions of interest nor the ability to perform interventions. For this reason, there has been much interest in active robotic capsules.

Many proposed magnetic microrobots have the potential to be used within lumina [17], [18]; however, we will restrict our attention here to devices that are comparable in size to the lumen itself and account for the existence of the lumen walls. The different forms of magnetic locomotion in lumina proposed to date can be classified into three main types: periodic, screw-like, and pulling. Periodic gaits are often biomimetic [19]–[21], whereas it is only through the use of applied magnetic fields that screw-like and pulling locomotion are possible.

Periodic locomotion refers to gaits that can be characterized by a cycle. Types of periodic locomotion include inchworm and undulatory gaits (which are not always separated by a clear distinction). Inchworm motion involves two feet taking turns anchoring to a surface as the body deforms to propel the robot forward. This type of motion can be created with soft and rigid robots. A concept from Kim *et al.* [10] uses a spatially uniform rotating magnetic field for actuation of a robot comprising two asymmetric magnetic elements separated by a compliant structure, as well as additional mechanical elements that are required to transduce the magnetic interaction into locomotion and prevent the magnetic elements from sticking together. Gaits representative of undulatory (traveling-wave) motion

have also been examined for use in a lumen. Nam *et al.* [22] described a magnetic-actuation concept that utilizes a uniform oscillating field to generate traveling-wave-type locomotion. The robot comprises a series of articulated magnetic segments with protruding legs to cause asymmetric friction with lumen walls when actuated by an oscillating magnetic field. It is worth noting that Kim *et al.* [23] developed a similar concept utilizing a uniform magnetic rotating field to develop a snake-like gait, but their motivation was explicitly non-lumen environments (i.e., surfaces). Due to the mechanical complexity of the respective designs, neither are inherently scalable. Diller *et al.* [24] created traveling-wave locomotion by continuously varying the magnetization throughout the body of a soft robot and actuating it using uniform magnetic fields. Building on this concept, [25] and [26] demonstrated multiple gaits, shapes, and material magnetizations for various mesoscale prototypes.

By placing a screw-like helical structure on the outside of a robotic device (e.g., capsule endoscope), magnetic torque can be directly converted into forward/backward propulsion in a lumen. This has been the most explored method for untethered endoluminal robots to date [27]–[31]. Because this method requires continuous rotation of the robot, it has only been applied to fully untethered devices. Incorporation into continuum devices or tethered capsule-like devices would be nontrivial.

Finally, magnetic forces can be utilized directly to manipulate a robotic device by pulling. To date, this has primarily been limited to application in magnetic capsule endoscopy of the colon [32]–[34], which is a relatively large lumen. However, it is well known that actuation methods based on magnetic torque tend to scale better than those based on magnetic force as the distance between the magnetic-field source and the actuated device increases [35].

III. Locomotion Model

In order to gain insight into the proposed locomotion mechanics, we use a simplified numerical model that we first introduced in [8], which has higher fidelity than the model we originally used in [7]. Herein, the robot body is modeled as a compliant beam with a magnet and thin rigid foot on each end. The magnetic forces and torques between all three magnets in the system are modeled explicitly [36]. All magnets are assumed to be perfect dipoles. Each of the magnets has a magnetic dipole $\boldsymbol{m}$ that points along the axis of the magnet. When a magnetic dipole $\boldsymbol{m}$ is placed in a magnetic field $\boldsymbol{b}$, a torque $\boldsymbol{\tau}$ is induced, which attempts to align the dipole with the applied field, and a force $\boldsymbol{f}$ is induced due to the spatial derivative in the applied field, which attempts to translate the dipole to a location with a stronger field:

$$\boldsymbol{\tau} = \boldsymbol{m} \times \boldsymbol{b} \tag{1}$$

$$\boldsymbol{f} = (\boldsymbol{m} \cdot \nabla)\boldsymbol{b}. \tag{2}$$

The dipole field generated by some actuator dipole $\boldsymbol{m}_a$ at each point in space represented by displacement vector $\boldsymbol{p}$ is

$$\boldsymbol{b}(\boldsymbol{p}) = \frac{\mu_0}{4\pi \|\boldsymbol{p}\|^5}\left(3\boldsymbol{p}\boldsymbol{p}^\top - I\|\boldsymbol{p}\|^2\right)\boldsymbol{m}_a. \tag{3}$$

TABLE I
Environment, Robot, and Actuator Parameters for Simulations and Experiments for the Three Robots Considered in This Article. *Not Considered in the Simulations. †In Tubes, "Floor" Indicates the Bottom of the Lumen

Parameter	Units	Thin Feet	Small	Capsule
Acceleration of gravity	$\mathrm{m{\cdot}s^{-2}}$	9.81	9.81	9.81
Env. permeability	$\mathrm{H{\cdot}m^{-1}}$	1.257e-6	1.257e-6	1.257e-6
Env. lumen diameter	mm	12	6	27
Coefficient of friction*		0.3	1.4	0.5
Rob. weight	g	0.438	0.30	4.05
Rob. body length	mm	30	14	25
Rob. foot length*	mm	0.53	2.5	5
Rob. body diameter	mm	2.5	2.5	5
Rob. lumen	mm	1×1	1×1	2×1
Rob. foot diameter	mm	10	5	12
Rob. elastic modulus	Pa	3.37e5	3.37e5	3.37e5
Rob. dipole moment	$\mathrm{A{\cdot}m^2}$	0.0110	0.0110	0.210
Act. to floor distance†	mm	137	137	200
Act. dipole moment	$\mathrm{A{\cdot}m^2}$	40	40	205

The lumen environment is represented as a rigid ceiling and floor, with which the feet and body make and break contact. A simplified friction model assumes perfect stiction between the foot and ceiling/floor with the largest contact force and no friction on the other (moving) foot. The actuator magnet drives the motion of the robot. To capture the gait of the robot, the rotation of the actuator magnet is discretized and a quasistatic iterative approach is used. For each actuator-magnet pose, the static equilibrium of the robot is found iteratively as follows:

1) compute intermagnet forces and torques;
2) compute deformation of the robot body, modeled with simple beam theory;
3) add the geometric constraint of the thin rigid feet to the deformed beam;
4) find the highest reaction force between the six potential points of contact with the environment; and finally
5) hold fixed the point of contact with the highest reaction force when determining the robot pose.

Once the solution for the robot's pose has converged, the pose of the actuator magnet is advanced by a small angle, and the process is repeated.

In order to validate the model's ability to predict the robot's deformation and locomotion, we fabricated a robot prototype with thin rigid feet and low friction to closely match the assumptions in the model. The robot is shown in Fig. 2 with parameters in the "Thin Feet" column of Table I. Experimental validation was performed using an omnidirectional electromagnet known as an Omnimagnet [37] as shown in Fig. 3(Ci). The dipole was chosen to be the strongest dipole that could be rotated using the Omnimagnet and the distance was selected as being neither too close (which would cause the robot to be stuck to the top of the tube) nor too far (which would result in the robot not being actuated properly). As illustrated in Fig. 2 and Supplementary Movie S1, the experimental and simulated robots move synchronously, demonstrating that the simulation is capturing the underlying physics of the locomotion method.

Using our model, we are able to reconsider the four magnetic-actuation configurations originally considered in [7], which include embedding the magnets with alternating or

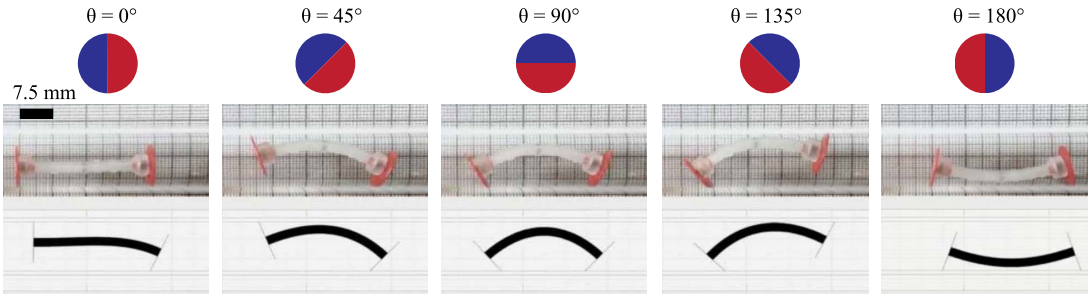

Fig. 2. Comparison of experimental (middle row) and simulated (bottom row) locomotion of thin-footed soft robot over half a cycle of dipole rotation (top row). The size of the rotating dipole, and its distance from the lumen, are not shown to scale.

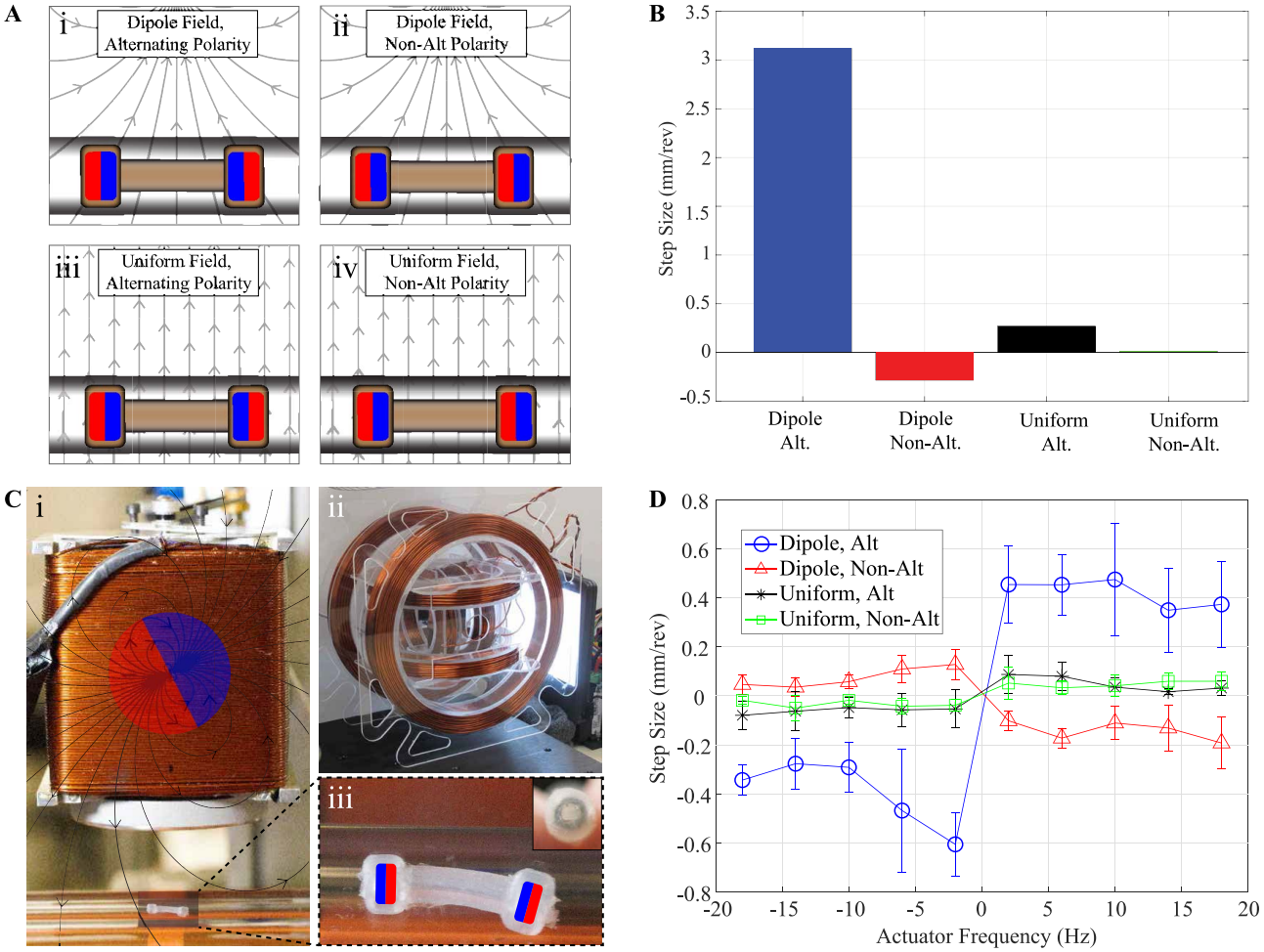

Fig. 3. Effects of magnetic field type and embedded-magnet polarity on crawling velocity. (**A**) Robots in four different configuration of embedded-magnet polarities and actuator-field types. (**B**) Simulated soft-robot step size per actuator-magnet revolution, for each configuration, using the simulation developed in [8]. (**C**) Experimental setup used in [7], showing (i) setup for rotating dipole fields using an Omnimagnet, (ii) setup for rotating uniform fields using tri-axial Helmholtz coils, and (iii) soft robot crawling through a tube, with an inset showing the robot's internal lumen. (**D**) Experimental data of robot step size at various actuator-field rotational frequencies, summarizing the complete experimental results of [7]. The mean step sizes are shown, along with their 95% confidence intervals, using the sign convention of Fig. 1.

non-alternating polarity and actuating with dipole or uniform magnetic fields, as shown in Fig. 3(A). The robot starts directly underneath the actuator magnet and then travels outwards once actuated. The simulation results shown in Fig. 3(B), which use the parameters in the "Small" column of Table I, demonstrate that our proposed rotating dipole field combined with embedded magnets of alternating polarity results in locomotion that is substantially more efficient than other configurations considered. Only our proposed configuration properly synchronizes the body deformation with the anchoring and releasing of the contact points.

Figure 3(D) presents the combined experimental results of [7]. Although there are quantitative differences from the results of Fig. 3(B) due to the assumptions of the model, such

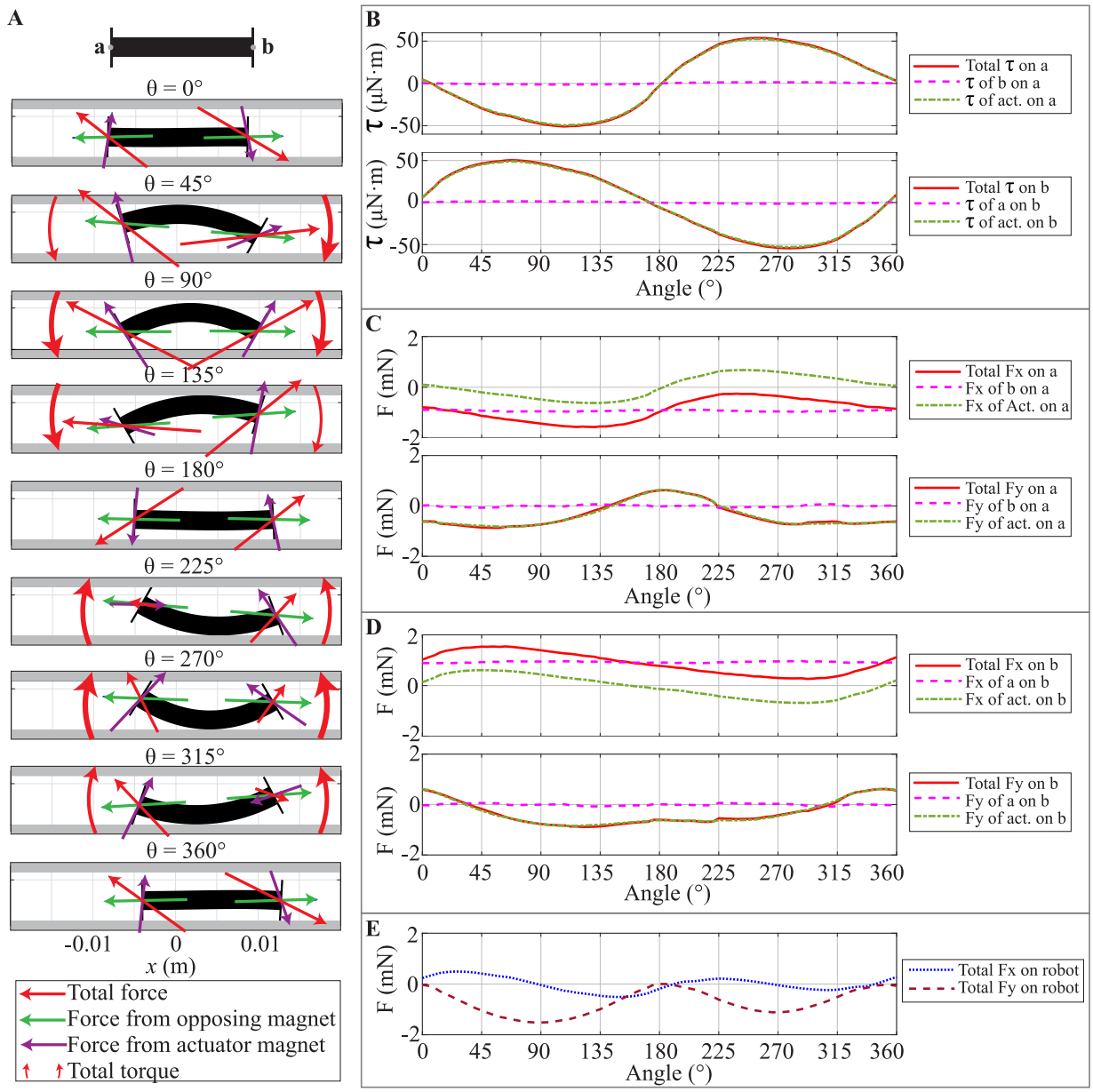

Fig. 4. Simulated locomotion of a soft robot through one cycle. (**A**) The gait of the robot with dipole-dipole interaction forces represented with arrows at points **a** and **b**; the length of the force vectors are scaled to relative force. Also shown is the total torque caused by the dipole-dipole interactions; the thickness of the torque arrows are scaled to relative torque magnitude. (**B**) The torques at points **a** and **b**. (**C**) The forces in the x and y direction on point **a**. (**D**) The forces in the x and y direction for point **b**. (**E**) The total force from the dipole-dipole interaction on the soft robot.

as thin feet and simplified friction, we see that the trends observed experimentally are the same, indicating that only our proposed configuration results in reliable locomotion in a deterministic direction.

Finally, we investigate the underlying physics of the proposed actuation method by examining the forces and torques on the robot throughout the gait cycle, which has yet to be done in previous work. The dipole-dipole interactions cause alternating feet to stick and slip. As the distance between the feet changes due to bending, the repeated action causes motion in a deterministic direction. We refer to the gait as inchworm-like, since there is an anchor-pull phase and an anchor-push phase. Figure 4 depicts an example of the robot's locomotion over one full rotation of the actuator magnet. It can be seen in Figs. 4(A–B) that the torques on foot **a** and **b** are asymmetric. This is the primary driver of the robot's gait; the asymmetric torques lead to a higher normal reaction force on one foot compared to the other. When the body deforms due to the torques, the foot with the lower reaction force will move while the other remains stationary. The magnetic forces on each foot are shown in Figs. 4(C–D). With sufficient separation between the actuator magnet and the robot, the forces do not significantly affect the gait of the robot. However, if the actuator magnet is too close to the robot, the forces may dominate the gait and reduce the locomotion efficiency. For example, Fig. 4(E) shows that the total force on the robot has

a relatively large vertical component; if the forces get too high, the robot will be held against the ceiling.

During one rotation of the actuator magnet, the robot goes through two anchor-pull anchor-push phases. Between 0° and 90°, foot **b** is fixed and foot **a** is pulled toward it. Between 90° and 180°, foot **a** is fixed and foot **b** is pushed forward. The second half of the cycle follows the same pattern, but with body deformation in the opposite direction. Between 180° and 225°, foot **b** is fixed and foot **a** is pulled toward it. Between 225° and 360°, foot **a** is fixed and foot **b** is pushed forward.

IV. Experiments and Results

A. Robot Fabrication

All robots fabricated in this article follow the same basic process. First, a 3D-printed mold is created with the desired robot dimensions. The robot body length and size are determined by the application, such as the size of a capsule endoscope. The foot diameter, foot length, and internal lumen size are determined by the geometry of the robot's embedded magnets, comprising an outer diameter, inner diameter, and thickness, plus 1 mm of silicon to cover them. The robot magnets are annular permanent magnets (K&J Magnetics) with axial magnetization, which are placed, with alternating polarity, on a thin rod and set into the mold. The mold is then submerged in silicone (Dragon Skin 20, Smooth-On) and left to cure. Once cured, the robot is removed from the mold and then the rod is removed to create the internal lumen.

B. Effects of Orientation Error Between the Lumen Axis and the Plane of Dipole Rotation

In the nominal configuration depicted in Fig. 1(A), the axis of the lumen lies in the plane swept by the rotating dipole. We conducted an experiment to quantify robustness to alignment of the lumen out of that plane, which is a measure of robustness to orientation error. The experimental setup, shown in Fig. 5(A–B) with parameters shown in the "Small" column of Table I, uses an Omnimagnet rotating a dipole at 6 Hz, which is the fastest performing frequency based on [7] for this setup. Each trial had the robot start directly below the center of the Omnimagnet where it would be travel outward when actuated. Each angle offset of the tube was a clockwise rotation away from the nominal configuration, as seen in Fig. 5(B).

As shown in Fig. 5(C), the robot's velocity is symmetric with respect to rotation direction, with the speed decreasing as the lumen deviates from the plane of the rotating dipole. We find that the locomotion is quite robust to deviations up to 45°. These results demonstrate that locomotion can still be achieved when the orientation of the lumen at the robot's current location is not well known.

C. Capsule-Endoscope-Size Robot

In this section, we explore the application of the magnetic gait for capsule-endoscope-size robots applicable to the GI tract. The capsule-endoscope-size robot shown in Fig. 6(A) has corresponding dimensions in the "Capsule" column of Table I.

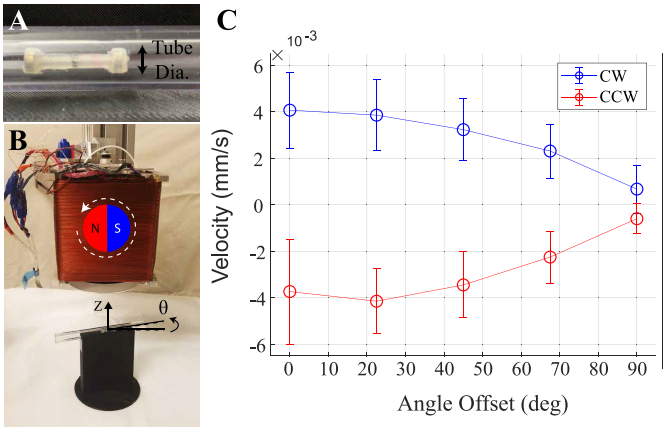

Fig. 5. Actuation misalignment experiment, with parameters shown in the "Small" column of Table I. (**A**) The soft robot. (**B**) The test setup comprising an Omnimagnet electromagnetic source with a dipole that rotates at 6 Hz, sweeping the plane of the image. The angle offset of the horizontal tube is varied by rotating the tube about the vertical z axis. (**C**) Robot's average velocity (mean with 95% confidence interval over 12 trials) as a function of tube orientation. The average velocity was determined by the distance the robot traveled after 6 seconds of actuation, starting from directly below the Omnimagnet.

It was modeled after existing clinical capsule devices [38], which at 12 mm in diameter and 25 mm in length is small enough to avoid getting stuck in the pylorus (rigid objects up to 20 mm in diameter) but still short enough to make the sharp turns of the intestines (rigid objects up to 50 mm in length) [39]. A single robot has the potential to be coupled with a second robot to form a longer two-component robot as shown in Fig. 6(B), potentially via directed self-assembly (more on this below). The two-component robot is 50 mm in length, and since it is not rigid, it should still be able to make the sharp bends of the intestine. To connect two robots they need to have alternating polarities, i.e., one needs to have magnet polarities pointing outward and the other needs to have polarities pointing inward, as shown in Fig. 6(B). Once connected, this robot will travel with an undulatory gait using the same principle of actuation as a single robot. Both the single robot and the two-component robot are tested in a synthetic bowel.

The experimental setup is shown in Fig. 6(C), with parameters shown in the "Capsule" column of Table I. The rotation of the actuator magnet is controlled by a stepper motor. The actuator magnet and stepper-motor assembly are attached to a gantry system to enable translation parallel to the lumen as the robot moves. The lumen environment used is a 305-mm-long synthetic intestine (SynDaver, Double-Layer Bowel). To create an internal cavity, the intestine is placed in a plastic support to keep it propped open. For this experiment, the actuator magnet is rotating at 2 Hz while translating at 8 mm/s. This combination was determined by trial and error to reliably move the robot through the bowel without any feedback of the location of the robot while keeping the actuator magnet approximately over the robot.

For both robot types, 30 trials were performed. In each trial, the robot started at one end of the bowel with the actuator magnet directly overhead. At the start of the trial, the

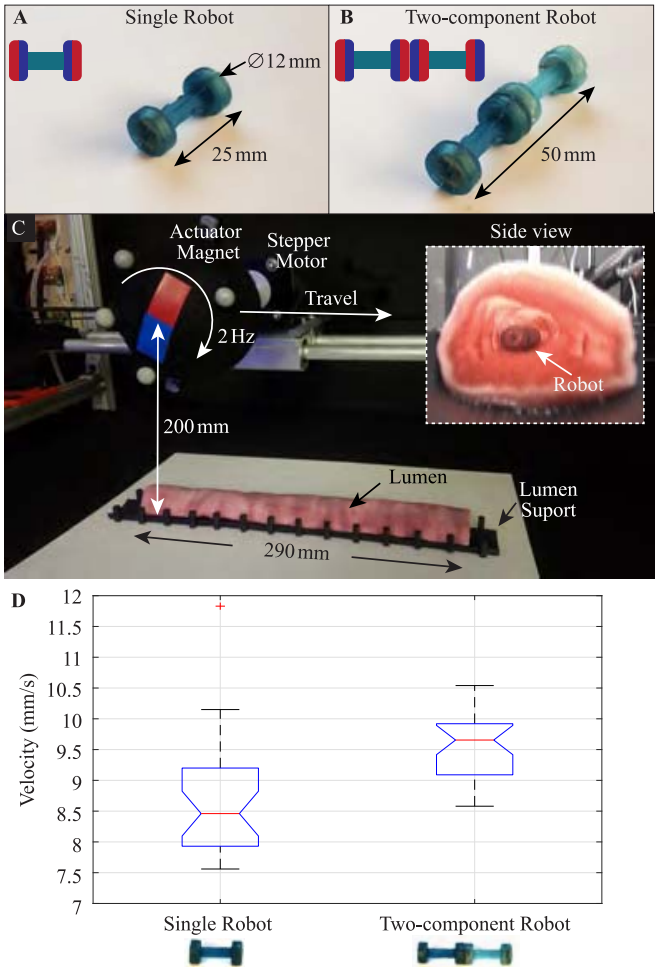

Fig. 6. Capsule-endoscope-size soft-robot experiments in synthetic bowels. (**A**) Single robot. (**B**) Two-component assembled robot. (**C**) Test setup with rotating actuator magnet mounted on a gantry system for linear translation of the actuator magnet parallel to the lumen. When the robot moves to the right the actuator-magnet rotation is clockwise, and vice versa. (**D**) Box-whisker plot of single robot and two-component robot velocities distribution over 30 trials. Notches indicate the 95% confidence intervals on the medians.

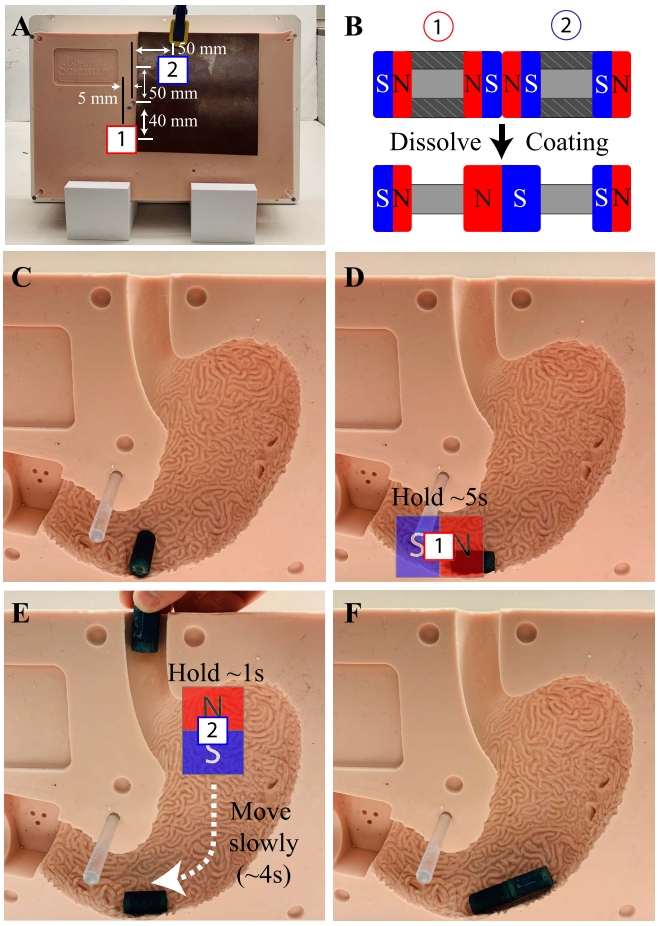

Fig. 7. Directed self-assembly. (**A**) Experiments were performed with the synthetic stomach with two halves held together using a plate and clamp. The numbers denote the initial location of the external magnet for each component drop. (**B**) For swallowing, components would be coated to have a smooth capsule shape. Once assembled, the coating on the robots would dissolve, enabling magnetic actuation. The two components have opposite magnetization, and the numbers correspond to the order that they were dropped into the stomach. The two center connected magnets are equivalent to a single magnet of the same size. (**C**) An example in which the first component is poorly oriented, without an external magnet. In this and the remaining images, we show only half of the synthetic stomach in order to visualize the components. (**D**) Using an external magnet held at position 1, the first component aligns in the ideal orientation when dropped. (**E**) The external magnet is then held at position 2 for 1 second after the second component is dropped, and is then moved slowly toward position 1. (**F**) An example of a successful assembly.

actuator magnet would start rotating and translating. The time it took the robot to travel to the other end was used to compute a mean velocity. For the single robot, the mean velocity was 8.7 mm/s with a standard deviation of 0.90 mm/s. For the two-component robot, the mean velocity was 9.5 mm/s with a standard deviation of 0.51 mm/s. The distribution of the trials is shown in Fig. 6(D). We observed a significantly faster speed ($p < 0.05$) with the two-component robot.

D. Directed Self-Assembly in a Synthetic Stomach

The two-component robot would enable larger, more complex robotic systems than would be feasible in a single-capsule paradigm, with the individual components swallowed and self-assembled inside the stomach (in addition to the improvement in locomotion efficiency discovered above). For example, each component could have a single dedicated function (e.g., imaging, localization). Nagy *et al.* [40] proposed magnetic self-assembly for such an application, in which each component had a permanent magnet on each end (as in our concept), but their magnets were diametrically magnetized (as opposed to the axial magnetization in our concept). As previously mentioned, self-assembly with our concept devices would require that each component have opposite magnetization of the segment proceeding it, which is also different than [40].

In this section, we explore the feasibility of self-assembly and directed self-assembly in the stomach. Our feasibility experiments are conducted in a synthetic stomach (The Chamberlain Group #2068). This stomach is made up of two halves that are held together by a plate and clamp, as shown in Fig. 7(A); in this state, the stomach is not visible, as would be the case for *in vivo* application. Since the robots are most likely to be coated in a rapidly dissolving substance (e.g., ice) for swallowing, cylindrical capsules were fabricated. The cylindrical capsules are 12 mm in diameter and 25 mm in

length, with 0.21 $A{\cdot}m^2$ (R622, K&J Magnetics) annular magnets at the ends. The first capsule has the two north poles pointing inward, and the second has the north poles pointing outward (Fig. 7(B)). The two robots were dipped into soapy water to simulate lubrication inside the stomach, and then dropped one at a time into the synthetic stomach. The assembly was recorded as either a success or a failure, with success defined as the intended axial connection between capsules and failure defined as any other connection (which typically manifested as a parallel connection between capsules).

The embedded magnets cause a rapid connection between the two components, with a pulling force of 4.5 N required to separate them. Since the small intestines have "crushing" forces of 1.6 N [41], this suggest that the two-component robot would not be pulled apart while traveling through the small intestines. If we consider that the holding force between two magnets scales quadratically with characteristic length, we could scale the down the characteristic length of the magnets by 40% and still maintain a connection.

We first considered self-assembly. For this experiment, the first component was dropped into the closed stomach, and after five seconds, the second component was dropped. For 100 trials, 70 were successful, for an estimated success rate of $70\pm9\%$ (95% confidence interval). This is likely not sufficient for clinical translation. For comparison, Nagy *et al.* [40] found the equivalent of a $74\pm12\%$ estimated success rate when using the best configuration of those that they considered.

Directed self-assembly is expected to significantly improve the rate of success by using an external magnetic field to influence the components during assembly. For example, without directed self-assembly, Fig. 7(C) shows how the first component can be oriented poorly, resulting in failed assembly when the second component is dropped. The external magnet used for directed assembly was a 20.3 $A{\cdot}m^2$ magnet (DX0X8, K&J Magnetics). As shown in Figs. 7(B, D), the external magnet was placed at position 1 against the wall of the closed model (i.e., with neither the stomach nor components visible to the experimenter), and held there for 5 seconds as the first component was dropped. The external magnet then moved directly outward to avoid unintentional movement of the first component. The external magnet was then moved to position 2. After the second component was dropped, the magnet was held in place for 1 second, catching the second component, and then moved slowly toward position 1 over the course of approximately 4 seconds. For 100 trials, 97 were successful, for an estimated success rate of $97 \pm 3\%$. This result, in which neither the external magnet nor the process have been optimized, suggests that directed self-assembly in the stomach holds great promise for this class of soft robot.

V. Discussion

The proposed concept is quite scalable in terms of fabrications. The soft-robot prototypes in this article were fabricated by embedding commercial annular permanent magnets into a polymer structure. We demonstrated three different sized robots: our smallest was 5 mm in diameter and 14 mm in length, and our largest had over double the diameter and nearly double the length. Although no attempt was made to optimize the design of these prototypes, they can still travel using the proposed method of actuation. Axially magnetized annular permanent magnets are commercially available with outer diameters as small as 1 mm. In addition, the recent demonstration of permanent magnets made through additive-manufacturing (i.e., 3D-printing) processes [42] suggest that our robots could be fabricated at smaller scales, which could also enable more than one internal lumen. However, one concern with significantly smaller robots is that the magnetic field experienced locally by the robot will become increasing homogeneous (since the robot's two magnets become closer to being at the same location), thus reducing locomotion efficiency. Determining the lower size limit on the effectiveness of the proposed actuation method is left as an open problem.

All of our robot prototypes had smooth surfaces. However, there is reason to believe that surface textures could be designed to improve the traction of the robot's feet, and thus improve the locomotion efficiency [43]. This is left as an open problem, but investigation of optimal texturing should be performed with correct environmental surface properties (e.g., mucus, compliance) in order to arrive at meaningful conclusions for clinical translation.

In our experiments and simulations, we set the distance between the actuator magnet and the lumen such that reliable locomotion was observed, but we have not attempted to find the optimal distance. However we know one must exist, since we know that locomotion becomes poor if the actuator magnet is either too far away or too close. This optimal distance is likely to be a function of the size of the actuator magnet. As a result, there may be an optimal combination of actuator-magnet size and distance for a given *in vivo* application.

In this article, we did not address localization or closed-loop control. In our prior works, we have developed localization methods that use sensors embedded in the robot to localize capsules, utilizing the same rotating magnetic field used for propulsion [31], [44]. Similar techniques could be applied here, although a variety of other techniques for localizing *in vivo* magnetic objects also exist.

It is our conjecture that our soft-robotic concept could be added to the distal end of a catheter or other continuum device to assist in insertion. As the catheter is inserted from the proximal end, the distal end could actively advance to reduce buckling or help guide and steer the catheter through more complex environments. It is almost certain that such an application of the concept would lead to improved insertion based on the results herein, but the degree of improvement is left as an open question. Going further, distributing many such elements along the length of a continuum device may lead to further improvement. The locomotion efficiency of the two-component robot compared to the single robot (Fig. 6) suggests that this may be the case. For continuum devices, our concept's optional internal lumen could potentially be used as a passageway for tools or fluids once the device has reached its desired location.

We demonstrated that directed self-assembly greatly improves successful connections between two robot components, compared to undirected self-assembly. For medical applications, the failure rate that we observed is likely still too high, but could be improved through a variety of mechanisms, including optimization of the method, and use of localization to ensure that the first component's orientation is correct (and correcting it if it is not) before assembling the second component. A means for disassembly has also not yet been considered, but such a method would mitigate the fear of incorrect assembly. We leave the above considerations as open problems.

We have begun to explore incorporating electroactive polymers, such as ionic polymer-metal composites (IPMC) into the bodies of our soft robots. Initial experiments incorporating a one-degree-of-freedom IPMC suggest that even better performance can be achieved if the soft body has this additional mechanism for controlled deformation [8]. This improved performance and additional capabilities provided by the IPMC warrants further investigation for tethered robots.

VI. Conclusion

In this article, we presented a magnetically actuated soft-robotics concept for use in untethered and tethered endoluminal applications, such as capsule endoscopes and catheters. The soft endoluminal robot is a simple device comprising two or more permanent magnets, axially magnetized and embedded co-axially with alternating polarity in a compliant body, with an optional internal lumen, actuated by an external rotating magnetic dipole field. We used simulations to elucidate the underlying physics of the proposed actuation concept. We combined simulations and experiments to demonstrate how the proposed concept outperforms other potential variants of the concept (which are similar to concepts that have been proposed in prior works). We experimentally demonstrated that locomotion is robust to misalignment between the soft robot and the applied field, which enables operation in different applications without precise knowledge of the robot's orientation or precise control of the actuator dipole field. Experiments were performed inside a synthetic bowel comparing a capsule-endoscope-size robot and a multi-component robot formed by connecting multiple capsule-endoscope-size robots axially. Finally, experiments in a synthetic stomach showed how the concept lends itself to directed self-assembly in the stomach, thus enabling multi-component robots that are larger than could be swallowed.

References

[1] Y. Fu, H. Liu, W. Huang, S. Wang, and Z. Liang, "Steerable catheters in minimally invasive vascular surgery," *Int. J. Med. Robot.*, vol. 5, no. 4, pp. 381–391, 2009.

[2] A. Loeve, P. Breedveld, and J. Dankelman, "Scopes too flexible··· and too stiff," *IEEE Pulse*, vol. 1, no. 3, pp. 26–41, Nov./Dec. 2010.

[3] J. Driller and E. H. Frei, "A review of medical applications of magnet attraction and detection," *J. Med. Eng. Technol.*, vol. 11, no. 6, pp. 271–277, 1970.

[4] E. H. Frei, "Medical applications of magnetism," *Critical Reviews in Solid State*, vol. 1. New York, NY, USA: CRC Press, 1970, pp. 381–407.

[5] L. J. Sliker and G. Ciuti, "Flexible and capsule endoscopy for screening, diagnosis and treatment," *Expert Rev. Med. Devices*, vol. 11, no. 6, pp. 649–666, 2014.

[6] G. Ciuti *et al.*, "Frontiers of robotic endoscopic capsules: A review," *J. Microbio. Robot.*, vol. 11, nos. 1–4, pp. 1–18, 2016.

[7] L. N. Pham and J. J. Abbott, "A soft robot to navigate the lumens of the body using undulatory locomotion generated by a rotating magnetic dipole field," in *Proc. IEEE/RSJ Int. Conf. Intell. Robot. Syst.*, Madrid, Spain, 2018, pp. 1783–1788.

[8] J. A. Steiner, O. A. Hussain, L. N. Pham, J. J. Abbott, and K. K. Leang, "Toward magneto-electroactive endoluminal soft (MEESo) robots," in *Proc. Dyn. Syst. Cont. Conf. ASME*, 2019, p. 9.

[9] D. Trivedi, C. D. Rahn, W. M. Kier, and I. D. Walker, "Soft robotics: Biological inspiration, state of the art, and future research," *Appl. Bionics Biomech.*, vol. 5, no. 3, pp. 99–117, 2008.

[10] S. H. Kim, S. Hashi, and K. Ishiyama, "Hybrid magnetic mechanism for active locomotion based on inchworm motion," *Smart Mater. Struct.*, vol. 22, 2012, Art. no. 027001.

[11] C. Majidi, "Soft robotics: A perspective—Current trends and prospects for the future," *Soft Robot.*, vol. 1, no. 1, pp. 5–11, 2014.

[12] C. Laschi, B. Mazzolai, and M. Cianchetti, "Soft robotics: Technologies and systems pushing the boundaries of robot abilities," *Sci. Robot.*, vol. 1, Dec. 2016, Art. no. eaah3690.

[13] J. Burgner-Kahrs, D. C. Rucker, and H. Choset, "Continuum robots for medical applications: A survey," *IEEE Trans. Robot.*, vol. 31, no. 6, pp. 1261–1280, Dec. 2015.

[14] E. H. Frei, J. Driller, H. N. Neufeld, I. Barr, L. Bleiden, and H. N. Askenazy, "The POD and its applications," *Med. Res. Eng.*, vol. 5, no. 4, pp. 11–18, 1966.

[15] Y. Kim, G. A. Parada, S. Liu, and X. Zhao, "Ferromagnetic soft continuum robots," *Sci. Robot.*, vol. 4, no. 33, 2019, Art. no. eaax7329.

[16] J. Jayender, R. V. Patel, and S. Nikumb, "Robot-assisted active catheter insertion: Algorithms and experiments," *Int. J. Robot. Res.*, vol. 28, no. 9, pp. 1101–1117, 2009.

[17] B. J. Nelson, I. K. Kaliakatsos, and J. J. Abbott, "Microrobots for minimally invasive medicine," *Annu. Rev. Biomed. Eng.*, vol. 12, pp. 55–85, Aug. 2010.

[18] M. Sitti *et al.*, "Biomedical applications of untethered mobile milli/microrobots," *Proc. IEEE*, vol. 103, no. 2, pp. 205–224, Feb. 2015.

[19] J. Gray, *Animal Locomotion*. New York, NY, USA: W. W. Norton Company, 1968.

[20] C. Gans, *Biomechanics: An Approach to Vertebrate Biology*. Ann Arbor, MI, USA: Univ. Michigan Press, 1974.

[21] S. Vogel, *Comparative Biomechanics: Life's Physical World*. Princeton, NJ, USA: Princeton Univ. Press, 2003.

[22] J. Nam, S. Jeon, S. Kim, and G. Jang, "Crawling microrobot actuated by a magnetic navigation system in tubular environments," *Sens. Actuat. A, Phys.*, vol. 209, pp. 100–106, Mar. 2014.

[23] S. H. Kim, S. Hashi, and K. Ishiyama, "Magnetic actuation based snake-like mechanism and locomotion driven by rotating magnetic field," *IEEE Trans. Magn.*, vol. 47, no. 10, pp. 3244–3247, Oct. 2011.

[24] E. Diller, J. Zhuang, G. Z. Lum, M. R. Edwards, and M. Sitti, "Continuously distributed magnetization profile for millimeter-scale elastomeric undulatory swimming," *Appl. Phys. Lett.*, vol. 104, Apr. 2014, Art. no. 174101.

[25] W. Hu, G. Z. Lum, M. Mastrangeli, and M. Sitti, "Small-scale soft-bodied robot with multimodal locomotion," *Nature*, vol. 554, pp. 81–85, Jan. 2018.

[26] T. Xu, J. Zhang, M. Salehizadeh, O. Onaizah, and E. Diller, "Millimeter-scale flexible robots with programmable three-dimensional magnetization and motions," *Sci. Robot.*, vol. 4, no. 29, 2019, Art. no. eaav4494.

[27] A. Chiba *et al.*, "Magnetic actuator for a capsule endoscope navigation system," *J. Magn.*, vol. 12, no. 2, pp. 89–92, 2007.

[28] J.-S. Lee, B. Kim, and Y.-S. Hong, "A flexible chain-based screw propeller for capsule endoscopes," *Int. J. Prec. Eng. Manuf.*, vol. 10, no. 4, pp. 27–34, 2009.

[29] H. Zhou, G. Alici, T. D. Than, and W. Li, "Modeling and experimental characterization of propulsion of a spiral-type microrobot for medical use in gastrointestinal tract," *IEEE Trans. Biomed. Eng.*, vol. 60, no. 6, pp. 1751–1759, Jun. 2013.

[30] A. W. Mahoney and J. J. Abbott, "Generating rotating magnetic fields with a single permanent magnet for propulsion of untethered magnetic devices in a lumen," *IEEE Trans. Robot.*, vol. 30, no. 2, pp. 411–420, Apr. 2014.

[31] K. M. Popek, T. Hermans, and J. J. Abbott, "First demonstration of simultaneous localization and propulsion of a magnetic capsule in a lumen using a single rotating magnet," in *Proc. IEEE Int. Conf. Robot. Autom.*, Singapore, 2017, pp. 1154–1160.

[32] G. Ciuti, P. Valdastri, A. Menciassi, and P. Dario, "Robotic magnetic steering and locomotion of capsule endoscope for diagnostic and surgical endoluminal procedures," *Robotica*, vol. 28, no. 2, pp. 199–207, 2010.

[33] M. Salerno, R. Rizzo, E. Sinibaldi, and A. Menciassi, "Force calculation for localized magnetic driven capsule endoscopes," in *Proc. IEEE Int. Conf. Robot. Autom.*, Karlsruhe, Germany, 2013, pp. 5334–5339.

[34] P. R. Slawinski, A. Z. Taddese, K. B. Musto, K. L. Obstein, and P. Valdastri, "Autonomous retroflexion of a magnetic flexible endoscope," *IEEE Robot. Autom. Lett.*, vol. 2, no. 3, pp. 1352–1359, Jul. 2017.

[35] J. J. Abbott *et al.*, "How should microrobots swim?" *Int. J. Robot. Res.*, vol. 28, nos. 11–12, pp. 1434–1447, 2009.

[36] J. J. Abbott, E. Diller, and A. J. Petruska, "Magnetic methods in robotics," *Annu. Rev. Control Robot. Auton. Syst.*, vol. 3, pp. 57–90, May 2020.

[37] A. J. Petruska and J. J. Abbott, "Omnimagnet: An omnidirectional electromagnet for controlled dipole-field generation," *IEEE Trans. Magn.*, vol. 50, no. 7, pp. 1–10, Jul. 2014.

[38] J. L. Toennies, G. Tortora, M. Simi, P. Valdastri, and R. J. Webster III, "Swallowable medical devices for diagnosis and surgery: The state of the art," *Proc. Inst. Mech. Eng. C, J. Mech. Eng. Sci.*, vol. 224, no. 7, pp. 1397–1414, 2010.

[39] T. E. Pavlidis, G. N. Marakis, A. Triantafyllou, K. Psarras, T. M. Kontoulis, and A. K. Sakantamis, "Management of ingested foreign bodies. How justifiable is a waiting policy?" *Surg. Laparosc. Endosc. Percutan. Techn.*, vol. 18, no. 3, pp. 286–287, 2008.

[40] Z. Nagy *et al.*, "Assembling reconfigurable endoluminal surgical systems: Opportunities and challenges," *Int. J. Biomechatronics Biomed. Robot.*, vol. 1, no. 1, pp. 3–16, 2009.

[41] M. Kamba, Y. Seta, A. Kusai, and K. Nishimura, "Comparison of the mechanical destructive force in the small intestine of dog and human," *Int. J. Pharm.*, vol. 237, nos. 1–2, pp. 139–149, 2002.

[42] Y. Kim, H. Yuk, R. Zhao, S. A. Chester, and X. Zhao, "Printing ferromagnetic domains for untethered fast-transforming soft materials," *Nature*, vol. 558, pp. 274–279, Jun. 2018.

[43] L. J. Sliker, M. D. Kern, J. A. Schoen, and M. E. Rentschler, "Surgical evaluation of a novel tethered robotic capsule endoscope using micro-patterned treads," *Surg. Endosc.*, vol. 26, no. 10, pp. 2862–2869, 2012.

[44] K. M. Popek, T. Schmid, and J. J. Abbott, "Six-degree-of-freedom localization of an untethered magnetic capsule using a single rotating magnetic dipole," *IEEE Robot. Autom. Lett.*, vol. 2, no. 1, pp. 305–312, Jan. 2017.